Heteroatom Chemistry
Volume 15, Number 7, 2004

Crystal Structures and Molecular Modeling of 1,8 Chalcogenide-Substituted Naphthalenes

Stephen M. Aucott, Heather L. Milton, Stuart D. Robertson, Alexandra M. Z. Slawin, and J. Derek Woollins

School of Chemistry, University of St Andrews, St Andrews, Fife, KY16 9ST, UK

Received 1 September 2004; accepted 8 September 2004

ABSTRACT: *The molecular structures of naphtho[1,8-cd][1,2]dithiole, naphtho[1,8-cd][1,2]diselenole, naphtho[1,8-cd][1,2]ditellurole, naphtho[1,8-cd][1,2]dithiole 1-oxide, naphtho[1,8-cd][1,2]dithiole 1,1-dioxide, and naphtho[1,8-cd][1,2]dithiole 1,1,2-trioxideand naphtho[1,8-cd][1,2]dithiole 1,1,2,2-tetroxide are compared. The E–E distance varies, broadly reflecting the degree of distortion imposed by the rigid naphthalene backbone as well as the degree of oxidation at sulfur.*

Index Entry:

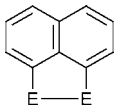

The naphthalene backbone imposes shortening of E–E bond lengths when E = S and Se compared to Ph—E—E—Ph systems but is itself subject to distortion as a consequence of the steric bulk of the E atoms. Heteroatom Chem 15:530–542, 2004; Published online in Wiley InterScience (www.interscience.wiley.com). DOI 10.1002/hc.20055

INTRODUCTION

Naphthalene-based systems are the simplest polycyclic aromatic hydrocarbons that allow substitution in a bay region (positions 1 and 8 of the naphthalene ring), (see Fig. 1). The extent of steric strain in peri-substituted (1,8-disubstituted) naphthalenes is dictated by the interaction between peri-substituents, which can be repulsive, bridged, or bonding. If there is no bonding, interaction between the two substantial steric strain is introduced. This strain can be released in various ways, e.g. by protonation in proton sponges [1]. Furthermore, the bidenticity combined with rigid C_3-backbone in bay-substituted naphthalenes is useful in the design of ligands for catalysis [2]. Obviously, the size of peri-atoms as well as the number and size of atoms attached to them are also important. In peri-diphospha-substituted naphthalenes with repulsive interactions between the peri-substituents, the steric strain is always significant [3]. The formation of a direct peri-atom–peri-atom bond [4] leads to partial relaxation of the strain. Phosphorus-substituted 1,8-diphosphinonaphthalenes have been studied by a number of groups, and Schmutztler recently reviewed his contribution [5]. There are a number of species available including $Nap(PCl_2)_2$ [6], $Nap[P(OMe)_2]_2$ [7], and $Nap[P(NR_2)_2]_2$ (R = Me, Et) [6,8]. We have used $NapP_2S_4$ for the generation of a range of new heterocycles [9,10], and we have recently discovered a relatively simple preparation of $NapP_2Cl_6$ [11].

In a comparative study, we utilized the increased nucleophilicity of phosphorus atom and lesser bulk of the OMe groups in $Nap[P(OMe)_2]_2$ in order to accomplish diselenation and selenation-sulfuration and investigate the extent of steric strain that can be induced [12] . Furthermore we have reported on halide-substituted systems [13]. In parallel with our

Correspondence to: J. Derek Woollins; e-mail: jdw3@st-and.ac.uk.

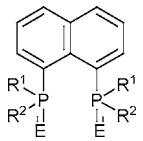

FIGURE 1 1,8 bay-substituted phosphorus system E = chalcogenide or lone pair.

studies on phosphorus-based systems, we have begun investigations into chalcogenide-based systems with the twofold aim of investigating the molecular structures and steric strains in the heterocycles and since sulfur/selenium rich species often demonstrate interesting intermolecular interactions in so-called molecular metals [14]. We have published some preliminary studies on the coordination chemistry of simple chalcogenide species [15]. Here we report a comparative study of a range of disubstituted systems as well as oxidized species (Fig. 2).

EXPERIMENTAL

Unless otherwise stated, manipulations were performed under an oxygen-free nitrogen or argon atmosphere using standard Schlenk techniques and glassware. Solvents were dried, purified, and stored according to common procedures. Naphtho[1,8-*cd*]-[1,2]dithiole [16], naphtho[1,8-*cd*][1,2]diselenole [16], naphtho[1,8-*cd*][1,2]ditellurole [17], naphtho-[1,8-*cd*][1,2]dithiole 1-oxide [18], naphtho[1,8-*cd*]-[1,2]dithiole 1,1-dioxide [19,20], naphtho[1,8-*cd*]-[1,2]dithiole 1,1,2-trioxide [21], and naphtho[1,8-*cd*][1,2]dithiole 1,1,2,2-tetroxide [22], were prepared according to literature methods.

Crystal Structure Analysis

Data (Table 1) were collected at 125 K on a Bruker SMART CCD diffractometer equipped with an Oxford Instruments low-temperature attachment, using Mo Kα radiation (λ = 0.71073 Å). Absorption corrections were performed on the basis of multiple equivalent reflections. In **3** the carbon atoms were refined isotropically. We examined several different crystals (including very small crystal sizes) under different experimental conditions. All of the datasets gave the same unit cell and crystal system but none of them was refinable anisotropically. In all other structures, the all nonhydrogen atoms were refined anisotropically. All refinements were performed by using SHELXTL (version 6.10, Bruker AXS, 2003). CCDC 236814–236820 contain the supplementary crystallographic data for this paper. These data can be obtained free of charge via www.ccdc.cam.ac.uk/conts/retrieving.html or from the Cambridge Crystallographic Data centre, 12 Union Road, Cambridge CB2 1EZ, UK; fax (+44) 1223-336-033; e-mail: deposit@ccdc.cam.ac.uk.

Semi-empirical PM3 calculations were performed using Spartan Pro.

RESULTS AND DISCUSSION

Figure 3 illustrates the idealized geometry for ortho- and peri-substituted systems. It should be noted that whilst the interatomic distance in ortho-substituted systems can vary as a consequence of the C–X bond length the idealized separation in peri-substituted systems is independent of X. The van der Waals radius of sulfur, selenium, and tellurium is 1.85, 2.00, and 2.20 Å respectively, so nonbonded peri-substituted systems would have to distort from the idealized geometry in the naphthalene by either splaying i.e. C—C—E angles varying from 120°; or by the naphthalene backbone becoming nonplanar. The situation for "simple" single-bonded systems improves somewhat. In Ph—E—E—Ph, the S—S, Se—Se, and Te—Te bond lengths are 2.030(5) [23], 2.29 [24], and 2.712(2) Å [25] respectively that compares with 2.0879(8), [2.096(3)], 2.3639(5), and 2.727(3)–2.734(3) (four independent molecules) Å in **1, 2**, and **3** respectively (Table 1, Figs. 4–6). It is clear from this observation that in the sulfur and

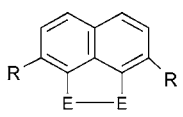

R = H, E = S **1,** E = Se **2,**

E = Te **3** , R = ^{t}Bu E = S **7**

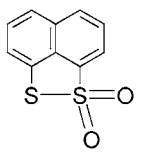

4

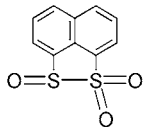

5

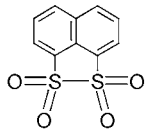

6

FIGURE 2 Compounds examined in this study.

TABLE 1 Details of Data Collections and Refinements

Compound	**1**	**2**	**3**	**4**	**5**	**6**	**7**
Formula	$C_{10}H_6S_2$	$C_{10}H_6Se_2$	$C_{10}H_6Te_2$	$C_{10}H_6S_2O_2$	$C_{10}H_6S_2O_3$	$C_{10}H_6S_2O_4$	$C_{18}H_{22}S_2$
Crystal habit	Orange prism	Red needle	Black needle	Pale yellow plate	Colourless prism	Colourless prism	Yellow prism
Crystal size (mm)	0.30 × 0.30 × 0.10	0.20 × 0.10 × 0.06	0.20 × 0.10 × 0.06	0.20 × 0.20 × 0.06	0.3 × 0.3 × 0.1	0.3 × 0.2 × 0.1	0.3 × 0.23 × 0.2
Crystal system	Monoclinic	Monoclinic	Orthorhombic	Monoclinic	Monoclinic	Triclinic	Orthorhombic
Space group	$P2_1/c$	$P2_1/n$	$Pna2_1$	$P2_1/n$	$C2/c$	P-1	$Pcca$
a (Å)	10.6495(16)	13.7575(19)	38.860(7)	8.820(2)	17.240(6)	7.957(3)	12.118(2)
b (Å)	10.6748(15)	4.2296(6)	15.492(3)	10.338(3)	8.095(3)	9.113(3)	12.010(2)
c (Å)	15.151(2)	15.396(2)	6.0647(11)	10.745(3)	15.132(5)	14.599(5)	11.2515(18)
α (°)	90	90	90	90	90	96.567(6)	90
β (°)	106.936(2)	110.205(2)	90	111.881(4)	120.496(5)	93.794(6)	90
γ (°)	90	90	90	90	90	106.021(6)	90
V (Å^3)	1647.6(4)	840.7(2)	3651.1(11)	909.1(4)	1819.7(11)	1005.5(6)	1637.5(5)
ρ_{calcd}	1.534	2.244	2.775	1.624	1.739	1.680	1.227
No. of reflections							
Measured	6760	3991	18399	4258	3582	5018	7232
independent	2313	1512	6539	1257	1260	2820	1138
Observed ($I > 2\sigma(I)$)	1915	1339	4488	1057	1140	2226	773
μ (mm^{-1})	0.574	8.725	6.327	0.549	0.563	0.522	0.314
max/min transmission	1.00000, 0.877064	1.00000, 0.654640	1.00000, 0.506992	0.42128, 0.34378	1.00000, 0.704527	1.00000, 0.611707	0.3061, 0.2105
No. of parameters	263	110	234	127	137	289	93
R (F^2, all data)	0.0350	0.0227	0.1212	0.0598	0.0483	0.0796	0.0682
wR (F^2, all data)	0.0669	0.0604	0.1594	0.1292	0.1149	0.1696	0.0929
Max. $\Delta\rho$ (eÅ^{-3})	0.214	0.402	2.075	0.658	1.120	1.332	0.142

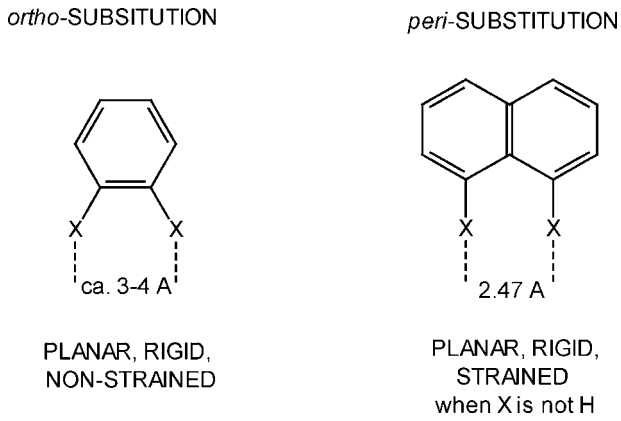

FIGURE 3 Comparison of geometry in disubstituted benzene versus naphthalene.

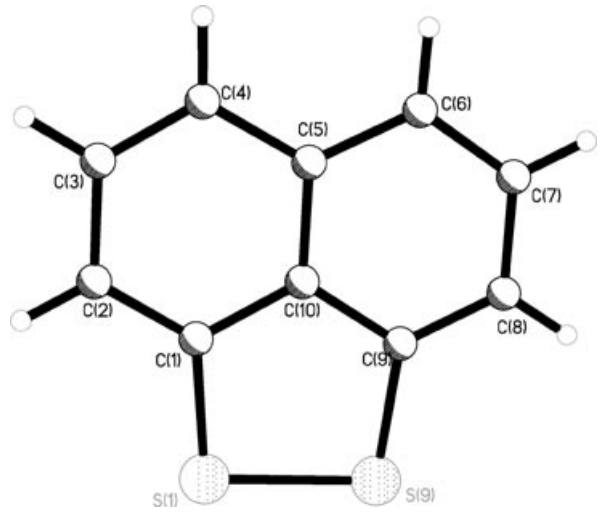

(a)

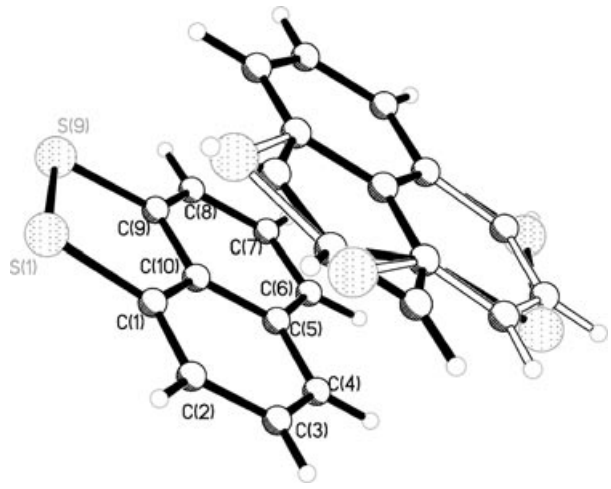

(b)

FIGURE 4 The X-ray structure of **1** (a) individual molecule with the atom numbering scheme and (b) two independent molecules illustrating the disorder in the second molecule.

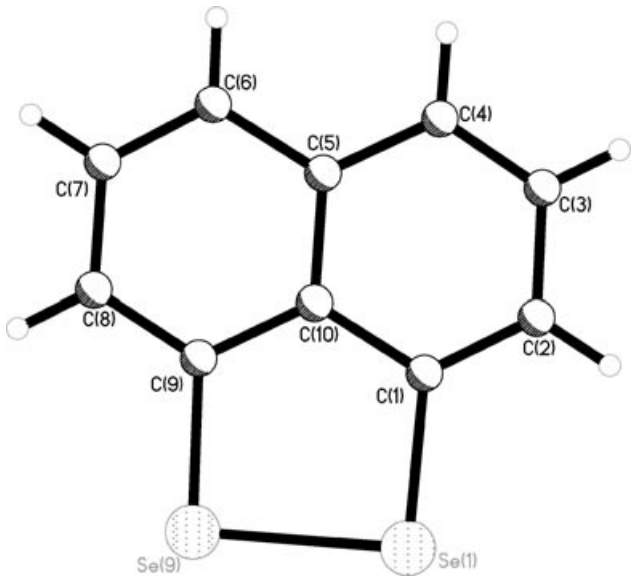

FIGURE 5 The X-ray structure of **2**.

selenium cases at least the 1,8 disubstitution imposes a lengthening of the E—E bond; though it is surprising that the Te—Te bond length is longer in **3** than in the "unconstrained" Ph—Te—Te—Ph. As mentioned above, peri-substitution imposes steric demands, these are relieved in **1** by a large negative splay angle and rather modest distortions from the plane of the naphthalene rings by the sulfur atoms, whereas **2** has a much reduced splay distortion and **3** has a positive splay angle and severe distortion from

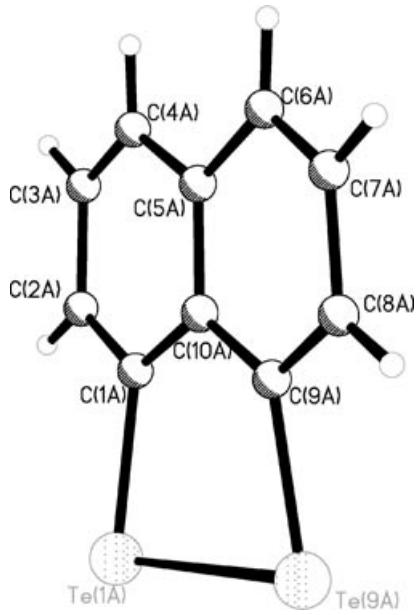

FIGURE 6 The X-ray structure of one of the independent molecule in **3**.

the naphthalene mean plane for the tellurium atoms. In **7**, it can be seen that adding bulky groups to the naphthalene backbone itself results in a more negative splay angle, with an small contraction of the S···S bond length (which may be as a consequence of the inductive electronic effect or steric compression), but that it does not result in very large distortions in the naphthalene itself. The naphthalene backbones of **1–3** themselves do show some distortion from planarity. The C(4)—C(5)—C(10)—C(1) torsion angles (0.7, 1.3, and 3.0° respectively) show the increasing distortions in the naphthalene backbones. As expected, the largest distortion results from the need to alleviate strain caused by the large tellurium atoms in **3**. The C(4)—C(5)—C(10)—C(9) torsion angles (179.4, 178.7, and 179.63°) are comparable with a number of those seen other types of naphthalene system in the CDS.

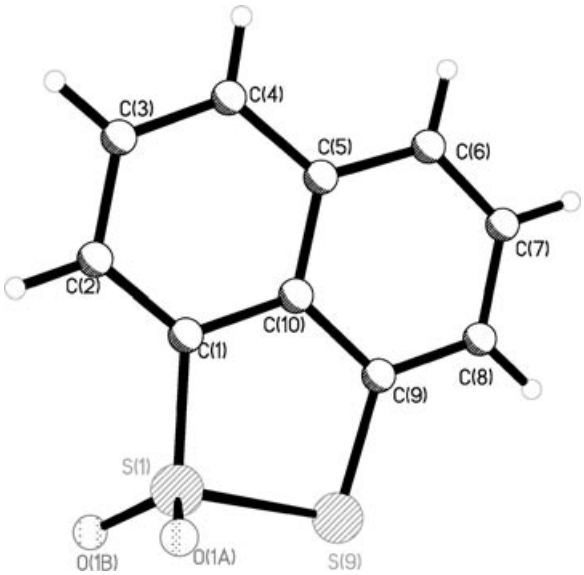

(a)

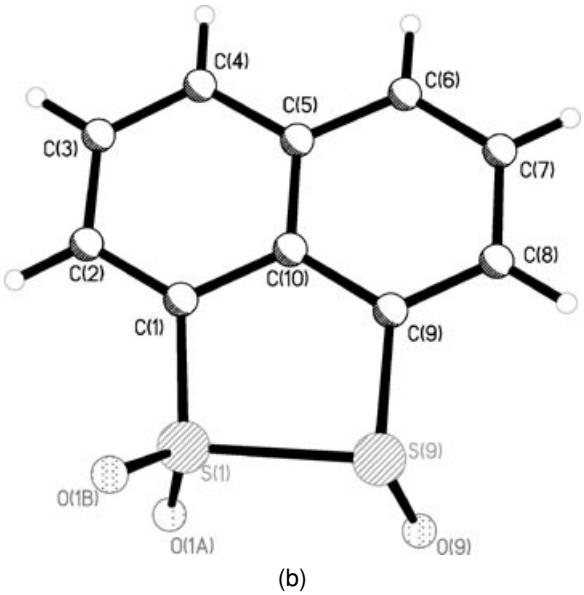

(b)

FIGURE 7 The X-ray structure of (a) **4** (b) **5** (c) **6**, and (d) **7**.

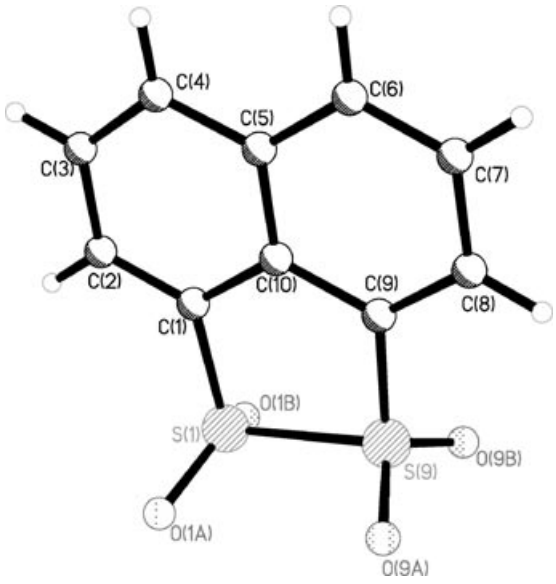

(c)

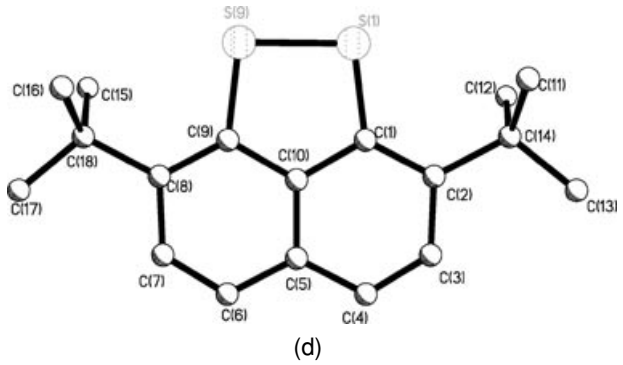

(d)

FIGURE 7 (Continued)

It is interesting to note that the C—C—E angles are close to 90° in all of the structures reported here—and indeed as the splay distortion is reduced, these angles are obliged to become closer to 90° if there is no puckering of the C_3E_2 ring.

The C—E distances in **1–3** (1.7619, 1.914, and 2.068 Å) are comparable with those in PhEEPh (1.79, 1.93, and 2.081 Å), whilst within the naphthalene backbones the C—C bond lengths show some alternation. This effect is known in other naphthalene systems [12,13], with C(1)—C(2), C(3)—C(4), C(6)—C(7), and C(8)—C(9) being noticeably shorter than the other C—C bonds. (The disorder in **1** does not allow us to make detailed discussions of its bond lengths.)... Sequential oxidation of the sulfur atoms

TABLE 2 Selected Crystallographic Bond Lengths (Å) and Angles (°) for **1–7** (Values in Parentheses are for Independent Molecules)

Compound	**1**	**2**	**3**	**4**	**5**	**6**	**7**
Formula	$C_{10}H_6S_2$	$C_{10}H_6Se_2$	$C_{10}H_6Te_2$	$C_{10}H_6S_2O_2$	$C_{10}H_6S_2\ O_3$	$C_{10}H_6S_2O_4$	$C_{18}H_{22}S_2$
				Peri-region distances			
E(1)–C(1)	1.7619(19) [1.813(4)]	1.914(3)	2.141(18) [2.13(2)] [2.09(2)] [2.13(2)]	1.762(3)	1.767(3)	1.770(5) [1.757(5)]	1.759(2)
E(9)–C(9)	1.7591(18) [1.7750(18)]	1.907(3)	2.14(2) [2.18(2)] [2.11(3)] [2.10(2)]	1.768(3)	1.790(3)	1.742(5) [1.745(5)]	1.759(2)
E(1)···E(9)	2.0879(8) [2.096(3)]	2.3639(5)	2.734(3) [2.727(3)] [2.731(3)] [2.730(3)]	2.1143(14)	2.2520(13)	2.2204(19) [2.251(2)]	2.0580(13)
				Naphthalene bond lengths			
C(1)–C(2)	1.373(3) [1.308(3)]	1.369(4)	1.38(3) [1.36(3)] [1.40(3)] [1.33(3)]	1.370(5)	1.359(5)	1.357(7) [1.364(7)]	1.390(3)
C(2)–C(3)	1.405(3) [1.434(6)]	1.419(4)	1.45(3) [1.43(3)] [1.39(3)] [1.38(3)]	1.406(5)	1.400(5)	1.397(8) [1.408(7)]	1.410(3)
C(3)–C(4)	1.364(3) [1.347(7)]	1.358(4)	1.26(3) [1.22(3)] [1.38(3)] [1.36(3)]	1.352(6)	1.380(5)	1.375(8) [1.370(7)]	1.352(3)
C(4)–C(5)	1.416(2) [1.389(5)]	1.418(4)	1.42(4) [1.40(3)] [1.40(3)] [1.44(3)]	1.407(5)	1.413(5)	1.415(7) [1.411(7)]	1.399(3)
C(5)–C(10)	1.415(3) [1.414(3)]	1.422(4)	1.40(3) [1.44(3)] [1.43(3)] [1.47(3)]	1.415(5)	1.408(5)	1.422(7) [1.420(7)]	1.404(4)
C(5)–C(6)	1.419(2) [1.409(3)]	1.429(4)	1.41(4) [1.43(3)] [1.43(3)] [1.39(3)]	1.437(5)	1.432(5)	1.403(7) [1.428(7)]	1.399(3)
C(6)–C(7)	1.376(3) [1.368(3)]	1.373(4)	1.34(3) [1.33(3)] [1.34(3)] [1.36(3)]	1.368(5)	1.366(5)	1.366(7) [1.363(7)]	1.352(3)
C(7)–C(8)	1.403(3) [1.401(3)]	1.407(4)	1.44(3) [1.40(3)] [1.36(3)] [1.38(3)]	1.404(5)	1.409(5)	1.412(7) [1.419(7)]	1.410(3)
C(8)–C(9)	1.372(3) [1.375(3)]	1.379(4)	1.39(3) [1.42(3)] [1.36(4)] [1.35(3)]	1.360(5)	1.380(5)	1.380(7) [1.375(7)]	1.390(3)
C(9)–C(10)	1.413(2) [1.410(3)]	1.409(4)	1.42(3) [1.40(3)] [1.44(4)] [1.47(3)]	1.399(5)	1.410(5)	1.418(7) [1.403(7)]	1.423(3)
C(10)–C(1)	1.413(2) [1.407(3)]	1.429(4)	1.41(3) [1.41(3)] [1.41(3)] [1.37(4)]	1.425(5)	1.418(5)	1.415(7) [1.419(7)]	1.390(3)

(Continued)

TABLE 2 Continued

Compound	**1**	**2**	**3**	**4**	**5**	**6**	**7**
S(1)–O(1A)	–	–	–	1.436(3)	1.427(3)	1.425(4) [1.421(4)]	–
S(1)–O(1B)	–	–	–	1.422(3)	1.435(3)	1.420(4) [1.423(4)]	–
S(9)–O(9A)	–	–	–	–	1.462(3)	1.439(4) [1.420(4)]	–
S(9)–O(9B)	–	–	–	–	–	1.424(4) [1.426(4)]	–
			Out-of-plane displacement				
E(1)	−0.0240 [−0.0377]	0.0516	0.2736 [−0.2822] [0.2606] [−0.2565]	−0.1180	−0.0637	0.0012 [0.0403]	0.0841
E(9)	−0.0245 [0.0230]	−0.0340	−0.2747 [0.2133] [−0.2290] [0.2178]	0.1692	0.0694	−0.0239 [−0.0153]	−0.0841
			Peri-region bond angles				
Splay angle[c]	−11.21 [−10.17]	−3.6	4.7 [5.1] [3.9] [4.3]	−11.4	−7.2	−8.6 [−7.6]	−13.48
E(1)–C(1)–C(10)	115.03(13) [114.01(19)]	116.9(2)	120.0(15) [120.1(17)] [122.0(17)] [120.2(19)]	116.2(2)	112.6(2)	113.6(4) [114.5(4)]	113.36(18)
E(9)–C(9)–C(10)	115.11(14) [117.84(14)]	117.4(2)	120.7(17) [119.0(17)] [117.9(19)] [119.1(16)]	113.0(3)	118.7(2)	115.3(4) [114.8(4)]	113.36(18)
C(1)–C(10)–C(9)	118.65(16) [117.98(18)]	122.1(3)	124(2) [126(2)] [124(2)] [125(2)]	119.4(3)	121.5(3)	122.5(4) [123.1(4)]	119.8(3)
E(1)–E(9)–C(9)	95.62(6) [93.84(11)]	91.71	85.8(7) [86.3(7)] [87.9(8)] [87.1(6)]	93.01(12)	89.63(11)	94.01(17) [94.09(18)]	96.47(7)
E(9)–E(1)–C(1)	5.56(6) [96.27(15)]	91.99	86.6(6) [86.8(6)] [85.4(7)] [86.3(7)]	96.89(12)	97.30(11)	94.56(17) [93.59(15)]	96.47(7)
C(1)–S(1)–O(1A)	–	–	–	108.9	111.8	111.7 [113.0]	–
C(1)–S(1)–O(1B)	–	–	–	113.0	111.3	111.6 [111.9]	–
C(9)–S(9)–O(9A)	–	–	–	–	109.1	110.8 [112.2]	–
C(9)–S(9)–O(9B)	–	–	–	–	–	112.4 [111.1]	–
O(1A)–S(1)–O(1B)	–	–	–	117.76(16)	118.65(16)	120.9(3) [120.2(2)]	–
O(9A)–S(9)–O(9B)	–	–	–	–	–	119.5(2) [121.5(3)]	–
			Central naphthalene ring torsion angles				
C(4)–C(5)–C(10)–C(1)	0.7(2) [0.3(3)]	1.3(4)	3.0	−1.3(5)	1.6(4)	0.1(6) [0.2(6)]	0.31(13)
C(4)–C(5)–C(10)–C(9)	−179.40(15) [−179.0(2)]	−178.7(3)	179.63	179.2(3)	−178.9(3)	−179.8(4) [1.6(7)]	−179.69(13)

TABLE 3 Bond Lengths and Angles from PM3 Calculations

	1	**2**	**3**	**4**	**5**	**6**	**7**
Formula	$C_{10}H_6S_2$	$C_{10}H_6Se_2$	$C_{10}H_6Te_2$	$C_{10}H_6S_2O_2$	$C_{10}H_6S_2O_3$	$C_{10}H_6S_2O_4$	$C_{22}H_{18}S_2$
				Peri-region distances			
E(1)–C(1)	1.762	1.876	2.144	1.776	1.778	1.775	1.764
E(9)–C(9)	1.762	1.876	2.144	1.754	1.785	1.775	1.764
E(1)–O(1)	–	–	–	1.451	1.474	1.479	–
E(1)–E(9)	2.104	2.409	2.889	2.229	2.355	2.415	2.099
				Naphthalene bond lengths			
C(1)–C(2)	1.372	1.363	1.363	1.375	1.375	1.375	1.379
C(2)–C(3)	1.415	1.415	1.414	1.413	1.413	1.413	1.421
C(3)–C(4)	1.371	1.371	1.370	1.370	1.369	1.369	1.369
C(4)–C(5)	1.421	1.422	1.421	1.421	1.421	1.421	1.421
C(5)–C(6)	1.421	1.422	1.421	1.422	1.422	1.421	1.421
C(6)–C(7)	1.371	1.371	1.370	1.369	1.369	1.369	1.369
C(7)–C(8)	1.415	1.415	1.414	1.415	1.414	1.413	1.421
C(8)–C(9)	1.372	1.363	1.363	1.372	1.372	1.375	1.379
C(9)–C(10)	1.426	1.410	1.411	1.429	1.427	1.428	1.427
C(10)–C(1)	1.426	1.410	1.411	1.424	1.425	1.428	1.427
C(10)–C(5)	1.403	1.410	1.414	1.405	1.407	1.408	1.402
S(1)–O(1A)	–	–	–	1.451	1.474	1.479	–
S(1)–O(1B)	–	–	–	1.451	1.464	1.479	–
S(9)–O(9A)	–	–	–	–	1.556	1.479	–
S(9)–O(9B)	–	–	–	–	–	1.479	–
				Out of plane displacement			
				Peri-region bond angles			
Splay angle	−15.51	−1.78	+10.86	−7.56	−4.04	−2.07	−11.71
E(1)–C(1)–C(10)	114.83	118.09	123.76	117.32	117.97	118.72	114.66
E(9)–C(9)–C(10)	114.83	118.09	123.76	115.90	117.78	118.72	114.66
C(1)–C(10)–C(9)	118.86	122.04	123.34	119.22	120.21	120.49	118.97
E(1)–E(9)–C(9)	95.74	90.89	84.57	95.08	91.67	91.04	95.86
E(9)–E(1)–C(1)	95.74	90.89	84.57	92.48	91.94	91.04	95.86
C(1)–S(1)–O(1A)	–	–	–	111.52	110.73	110.67	–
C(1)–S(1)–O(1B)	–	–	–	111.52	111.19	110.67	–
C(9)–S(9)–O(9A)	–	–	–	–	106.68	110.67	–
C(9)–S(9)–O(9B)	–	–	–	–	–	110.67	–
O(1A)–S(1)–O(1B)	–	–	–	115.49	115.98	116.29	–
O(9A)–S(9)–O(9B)	–	–	–	–	–	116.29	–
				Central naphthalene ring torsion angles			
C(4)–C(5)–C(10)–C(1)	0.00	0.00	0.00	0.00	−1.23	0.00	0.00
C(4)–C(5)–C(10)–C(9)	180.00	180.00	180.00	180.00	179.38	180.00	180.00

in **1** has little effect on the C–S bond lengths but results in significant increases in the S–S bond length and a gradual reduction in the splay angle distortion from **4–6**. This increase in the S–S bond length is seen in Ph–SO_2–S–Ph [26] and Ph–SO_2–SO_2–Ph [27]. The oxygen atoms in **4–6** are disposed above and below the naphthalene ring, which is in contrast to the platinum complexes where one of the oxygen substituents tends to be coplanar with the naphthalene ring. The S=O bonds in **4–6** are very similar (see Fig. 7). In **4**, S(1)–O(1A) is 1.436(3) and S(1)–O(1B) is 1.422(3). This pattern is also seen in **5** and **6**. There is however a slightly longer S(9)–O(9A) bond (1.462(3) Å) in **5**. This is related to intermolecular S—O interaction (discussed later). The sulfur atoms themselves are also displaced above and below the planes of the naphthalene backbones, but this deviation decreases with the increasing numbers of oxygen atoms. Where there are two oxygen atoms on a sulfur, the S atom adopts a distorted tetrahedral geometry. The C(1)–S(1)–O(1A) angle of 108.9° in **4** is very close to the ideal tetrahedral angle of 109.5°. However, the other angles around the sulfur atoms of **4, 5**, and **6** (shown in Table 2) have much more significant deviations from the ideal geometry.

We have compared our structural studies with molecular modeling. The geometric parameters for **1–7** are summarized in Table 3. The semi–empirical PM3 calculations show that the lengthening of the E–E bond in **1–3** is predictable, but the calculated

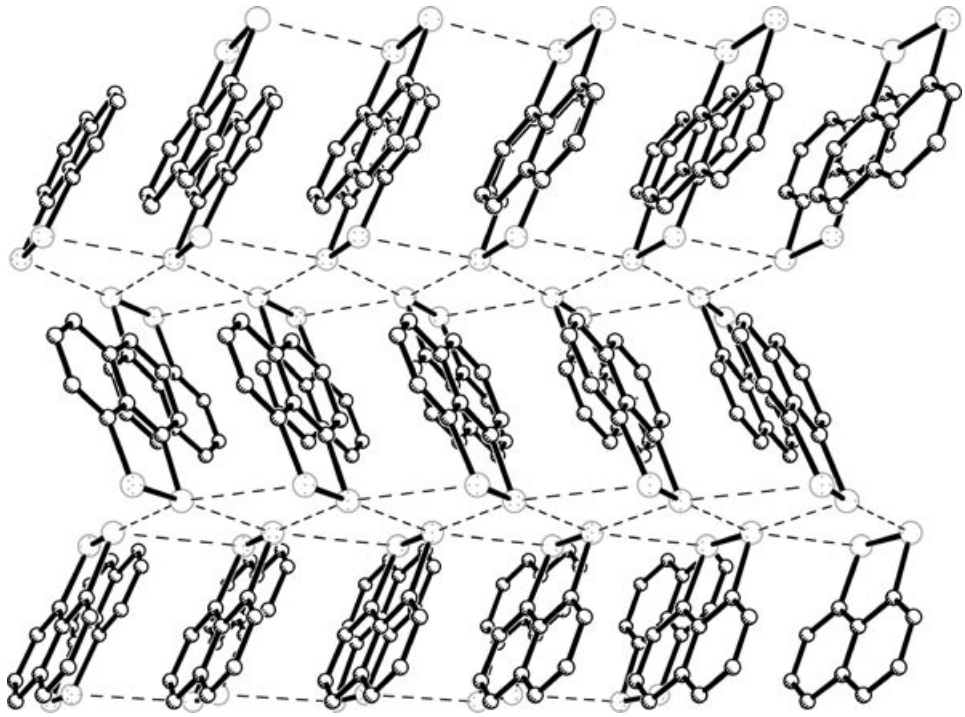

(a)

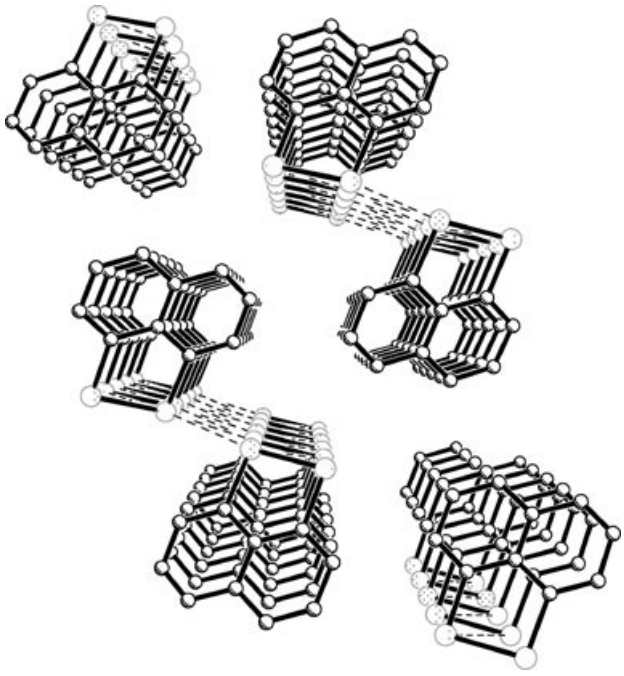

(b)

FIGURE 8 Packing of **2** (a) along the *c*-axis (b) along the *b*-axis.

values are generally longer than those in the crystal structures. The percentage difference between the actual E—E bond length and the calculated bond length increases as the size of the E atoms increases from **1** to **3**. This however is not the case where the C—E bond lengths are concerned. The calculated values are remarkably similar to those in the crystal structures (shown in Table 2). The calculated splay angles are also shown in Table 3. The general trend from negative to positive is predicted but, as with

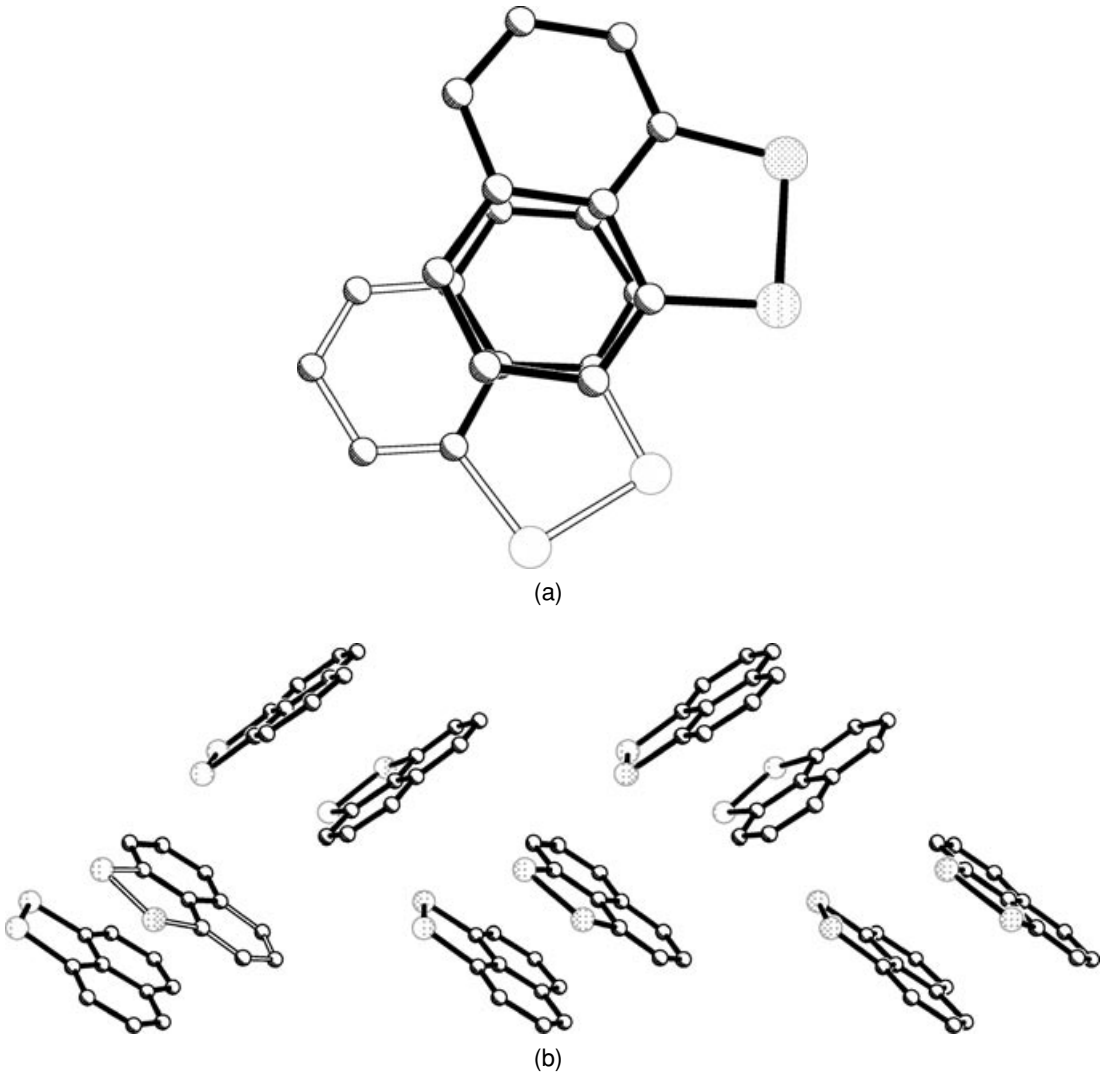

FIGURE 9 Packing of **1** (a) staggered overlap of two molecules and (b) overlapping π-stacks.

the calculated E—E distances, the percentage difference between the calculated and actual splay angles increases from **1** to **3**. The angular differences are considerably larger than the differences in the bond lengths. **7a** does show some disagreement with the observed structures as far as the splay angle is concerned. The calculations indicate that **7** should have a smaller splay angle than **1**, but Table 2 shows that in fact the opposite occurs.

The observed S—S bond lengths in **4–6** also follow the trend predicted from the calculations, but the observed bond lengths are all slightly shorter than the calculated values. The calculations also show a good agreement with the C—E bond lengths. The crystal structure of **6** shows that C(9)—S(9) and C(1)—S(1) are 1.770(5) and 1.742(5) Å respectively, while the calculations predict equal bond lengths of 1.775 Å. The PM3 calculations predict a small increase in the S=O bond lengths from **4–6**, but this is not seen in the crystal structures. Instead, the S=O bond lengths are reasonably consistent. As in the case of **1–3**, the calculated bond lengths tend to be slightly longer than the actual values. Despite this, the calculations do predict the general trends seen in the crystal structures. Table 3 shows that the calculations also predicted the pseudotetrahedral nature of the sulfur atoms, although comparisons with the X-ray structures show the calculated geometries to be nearer to the ideal geometry. As with **1–3**, the general trend in the splay angle is seen in the modeling results. As more oxygen atoms are added, the negative splay angle gets nearer to zero. As might be expected, the calculated geometries do show a much larger change in splay angle than the X-ray structures. Since the crystal structures show some deviations from 180° in the naphthalene torsion

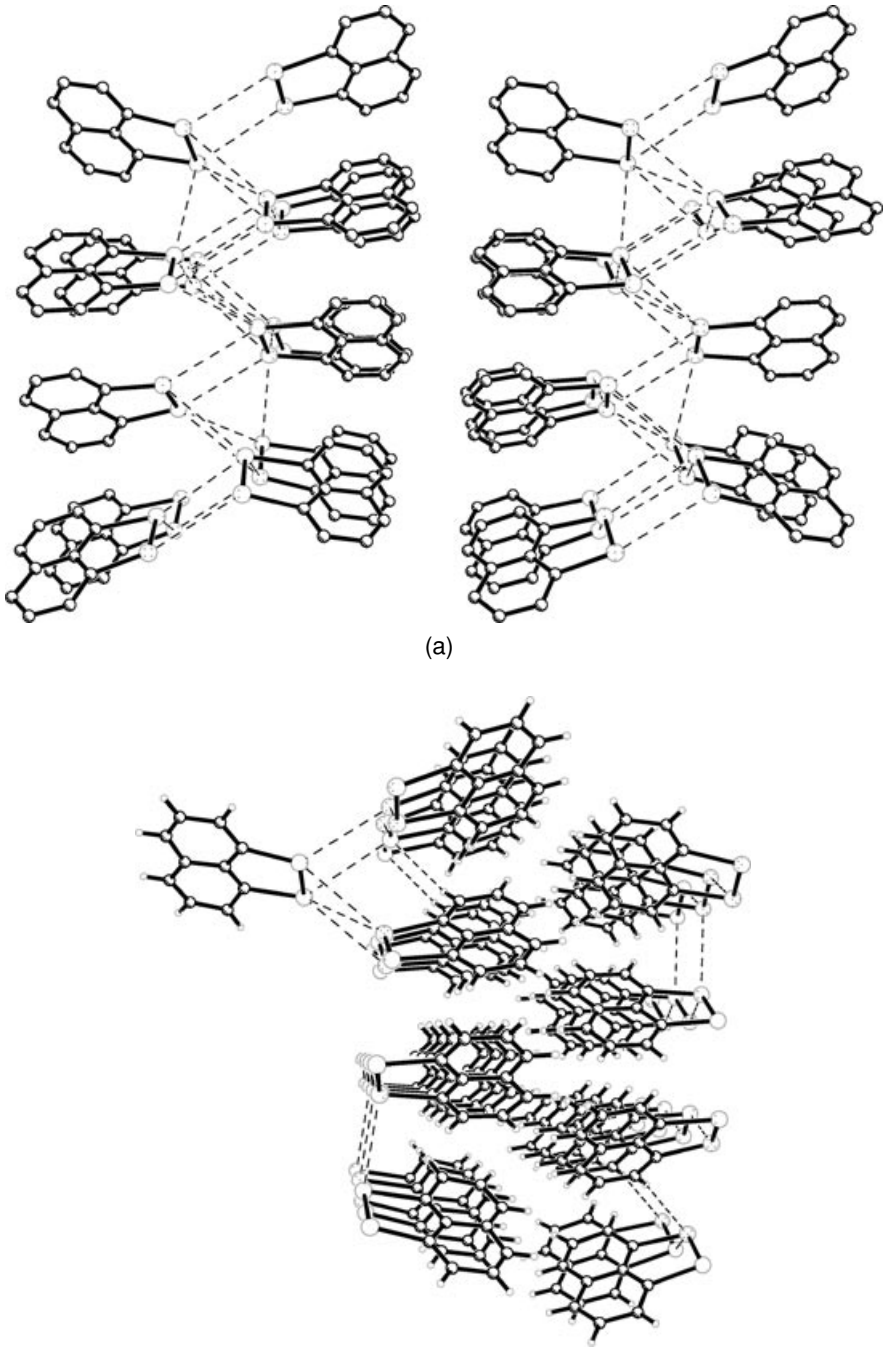

FIGURE 10 Packing of **3** (a) along the *c*-axis and (b) along the π-stacks.

angles, it was expected that similar deviations would be observed in the calculated structures. Table 3 shows that small deviations are indeed seen in **5a**, but there are no noticeable deviations in the other structures.

The solid-state structures of **1–3** show some interesting packing effects as a consequence of the high polarizability of the chalcogen atoms present. In **2**, the molecules form herringbone π-stacks with a π–π distance of 3.81 Å (Fig. 8a) with the π-stacks being inclined by 67.5° to one another. The stacks are linked by an Se···Se interaction as shown in Fig. 8b (Se(1)...Se(1′) 3.45 Å) In 1, there are two independent molecules per unit cell. Figure 9a shows that only one half of each naphthalene backbone overlaps in the stacks, with the sulfur atoms in a

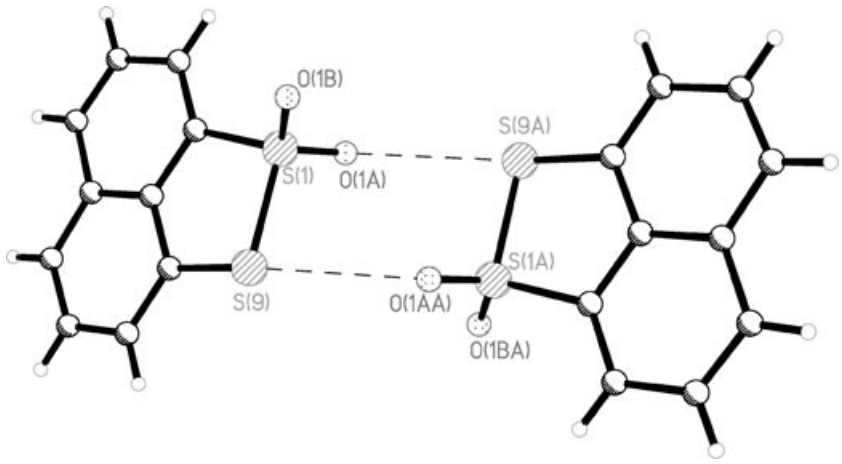

FIGURE 11 Intermolecular interactions in **4**.

staggered conformation (this is also seen in the low-occupancy disordered component). The interplanar separation of the two molecules is approximately 3.56 Å. Figure 9b shows the overlapping π-stacks. The four independent molecules in 3 are arranged at ∼40° to one another (Fig. 10a) with a number of intermolecular Te···Te interactions that lie in the range of 3.61–4.14 Å. The π–π distance in 3 is 4.12 Å, and the π-stacking is clearly shown in Fig. 10b.

In **4**, there are two intermolecular S···O interactions seen. The S(9)···O(1AA) and S(9A)···O(1A) distances are both 3.12 Å. This results in the dimer arrangement as seen in Fig. 11. **5** also has a number of intermolecular interactions present in its structure. The S(9)···O(1AA) and S(9A)···O(9AA) interactions (3.46 and 3.1 Å respectively) along with the O(1B)···O(9A) interaction result in chains of molecules as shown in Fig. 12. The steric bulk of the four oxygen atoms in **6** prevent any intermolecular S···O interactions, and no other meaningful interactions are observed. The steric bulk of the butyl groups present in **7** also prevent any meaningful intermolecular interactions.

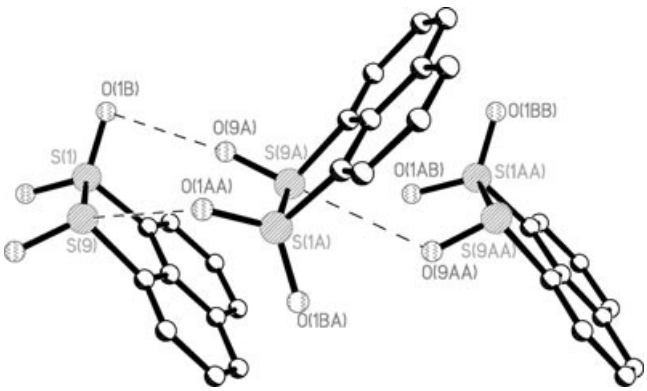

FIGURE 12 Intermolecular interactions in **5**.

REFERENCES

[1] See e.g. (a) Staab, H. A.; Kirsch, A.; Barth, T.; Krieger, C.; Neugebauer, F. A. Eur J Org Chem 2000, 1617–1622; (b) Raab, V.; Kipke, J.; Gschwind, R. M.; Sundermeyer, J. Chem Eur J 2002, 8, 1682–1693.

[2] (a) Jackson, R. D.; James, S.; Orpen, A. G.; Pringle, P. G. J Organomet Chem 1993, 458, C3–C4; (b) James, S. L.; Orpen, A. G.; Pringle, P. G. J Organomet Chem 1996, 525, 299–301.

[3] See e.g. (a) Kilian, P.; Slawin, A. M. Z.; Woollins, J. D. Eur J Inorg Chem 1999, 2327–2333; (b) Karacar, A.; Thonnessen, H.; Jones, P. G.; Bartsch, R.; Schmutzler, R. Chem Ber/Recueil 1997, 130, 1485–1489; (c) Karacar, A.; Freytag, M.; Jones, P. G.; Bartsch, R.; Schmutzler, R. Z Anorg Allg Chem 2001, 627, 1571–1581 and references therein.

[4] (a) Karacar, A.; Freytag, M.; Jones, P. G.; Bartsch, R.; Schmutzler, R. Z Anorg Allg Chem 2002, 628, 533–544; (b) Karacar, A.; Klaukien, V.; Freytag, M.; Thonnessen, H.; Omelanczuk, J.; Jones, P. G.; Bartsch, R.; Schmutzler, R. Z Anorg Allg Chem 2001, 627, 2589–2603; (c) Karacar, A.; Freytag, M.; Thonnessen, H.; Omelanczuk, J.; Jones, P. G.; Bartsch, R.; Schmutzler, R. Heteroatom Chem 2001, 12, 102–113.

[5] Karacar, A.; Freytag, M.; Jones, P. G.; Bartsch, R.; Schmutzler, R. Z Anorg Allg Chem 2002, 628, 533–544.

[6] Karacar, A.; Thonnessen, H.; Jones, P. G.; Bartsch, R.; Schmutzler, R. Chem Ber/Recueil 1997, 130, 1485–1489.

[7] Karacar, A.; Freytag, M.; Jones, P. G.; Bartsch, R.; Schmutzler, R. Z Anorg Allg Chem 2001, 627, 1571–1581.

[8] Karacar, A.; Freytag, M.; Thonnessen, H.; Jones, P. G.; Bartsch, R.; Schmutzler, R. J Organomet Chem 2002, 643–644, 68–80.

[9] Foreman, M. R. St. J.; Novosad, J.; Slawin, A. M. Z.; Woollins, J. D. J Chem Soc, Dalton Trans 1997, 1347–1350.
[10] (a) Kilian, P.; Slawin, A. M. Z.; Woollins, J. D. Eur J Inorg Chem 1999, 2327–2333; (b) Kilian, P.; Marek, J.; Marek, R.; Tousek, J.; Humpa, O.; Slawin, A. M. Z.; Touzin, J.; Novosad, J.; Woollins, J. D. J Chem Soc, Dalton Trans 1999, 2231–2236 and references therein.
[11] Kilian, P.; Slawin, A. M. Z.; Woollins, J. D. Eur J Inorg Chem, 2003, 249–254.
[12] Kilian, P.; Slawin, A. M. Z.; Woollins, J. D. Dalton Trans 2003, 3876–3885.
[13] Kilian, P.; Milton, H. L.; Slawin, A. M. Z.; Woollins, J. D. Inorg Chem, accepted.
[14] (a) Fitzmaurice, J. C.; Slawin, A. M. Z.; Williams, D. J.; Woollins, J. D. J Chem Soc, Chem Commun 1993, 1479–1480; (b) Martin, J. D.; Canadell, E.; Fitzmaurice, J. C.; Slawin, A. M. Z.; Williams, D. J.; Woollins, J. D. J Chem Soc, Dalton Trans 1994, 1995–2004; (c) Gimenez-Saiz, C.; Woollins, J. D.; Slawin, A. M. Z.; Coronado, E.; Martinez-Agudo, J. D.; Gomez-Garcia, C. J.; Robertson, N. Mol Cryst Liq Cryst 1999, 335, 43–52; (d) Gimenez Saiz, C.; Woollins, J. D.; Slawin, A. M. Z. Cryst Struct Eng 2002, 15–24.
[15] Aucott, S. M.; Milton, H. L.; Robertson, S. D.; Slawin, A. M. Z.; Walker, G. D.; Woollins, J. D. Chem Eur J, accepted.
[16] Yui, K.; Aso, Y.; Otubo, T.; Ogura, F. Bull Chem Soc Jpn 1988, 61, 953–959.
[17] Meinwald, J.; Dauplaise, D.; Wudl, F.; Hauser, J. J. J Am Chem Soc 1977, 99, 255–257.
[18] Oxelbark, J.; Thunberg, L.; Andersson, A.; Allenmark, S. Acta Chem Scand 1999, 53, 710–713.
[19] Zwieg, Hoffman, A. K. J Org Chem 1965, 30, 3997–4001.
[20] Kice, L.; Krowicki, K. J Org Chem 1981, 46, 4894–4898.
[21] Chau, M.; Kice, J. L. J Org Chem 1977, 42, 3265–3270.
[22] Chau, M.; Kice, J. L. J Org Chem, 1978, 43, 914–922.
[23] Lee, J. D.; Bryant, M. W. R. Acta Crystallogr 1969, B25, 2095–2101.
[24] Marsh, R. E. Acta Crystallogr 1952, 5, 458–462.
[25] Llabres, P. G.; Didenberg, O.; DuPont, L. Acta Crystallogr, Sect B 1972, 28, 2438–2444.
[26] Capato, R.; Palumbo, G.; Nardelli, M. Gazz Chim Ital 1984, 114, 421–430.
[27] Kiers, C. T.; Vos, A. Recl Trav Chim Pay-Bas (Fr.) 1972, 91, 126–132.